Talanta 82 (2010) 1809–1813

Contents lists available at ScienceDirect

Talanta

journal homepage: www.elsevier.com/locate/talanta

A simple colorimetric FIA method for the determination of pyrite oxidation rates

Owen D. Osborne[a], Allan Pring[a,b], Claire E. Lenehan[a,*]

[a] School of Chemical and Physical Sciences, Flinders University, Adelaide, Australia
[b] Department of Mineralogy, South Australian Museum, Adelaide, Australia

ARTICLE INFO

Article history:
Received 2 July 2010
Received in revised form 30 July 2010
Accepted 30 July 2010
Available online 10 August 2010

Keywords:
Pyrite
FIA
Flow analysis
Iron
5-Sulfosalicylic acid

ABSTRACT

A method for the rapid determination of the oxidation rate of naturally occurring pyrite (FeS_2) samples is presented. The progress of the oxidation reaction was followed by measurement of the concentration of total dissolved iron using flow injection analysis. Iron was determined using UV–vis detection after reaction with the colorimetric reagent 5-sulfosalicylic acid in the presence of ammonia. The calibration function was linear between 5 and 150 mg L^{-1}, and the detection limit was 0.46 mg L^{-1}. The relative standard deviation was typically less than 1% ($n = 10$) and the measurement frequency was 60/h. The method was used to quantify the oxidation rate of 10 ground and cleaned pyrite samples (53 μm < x < 106 μm) from various international locations that were subjected to accelerate oxidation in acidic hydrogen peroxide. Results of these experiments showed that there was almost an order of magnitude of difference in oxidation rates of the pyrite samples.

1. Introduction

Pyrite (FeS_2) is widely acknowledged as the most copious and widespread of the sulfide minerals on the Earth's surface [1–6]. It is a semiconductor [7] and is particularly abundant in its association with coals and base metal and gold ores [8] and its chemistry is important in mineral processing; particularly the liberation of refractory gold [9] and acid mine drainage [3]. Pyrite oxidation is autocatalytic in nature occurring via a series of reactions (Eqs. (1)–(3)). Initially, in the presence of atmospheric oxygen and water pyrite oxidises according to Eq. (1), secondly the ferrous ions produced by Eq. (1) are oxidised by atmospheric oxygen (Eq. (2)), and finally the resulting ferric ions act as an oxidising agent for pyrite (Eq. (3)).

$$2FeS_{2(s)} + 7O_{2(g)} + 2H_2O_{(l)} \rightarrow 2Fe^{2+}{}_{(aq)} + 4SO_4{}^{2-}{}_{(aq)} + 4H^+{}_{(aq)} \quad (1)$$

$$4Fe^{2+}{}_{(aq)} + O_{2(g)} + 4H^+{}_{(aq)} \rightarrow 4Fe^{3+}{}_{(aq)} + 2H_2O_{(l)} \quad (2)$$

$$FeS_{2(s)} + 14Fe^{3+}{}_{(aq)} + 8H_2O_{(l)} \rightarrow 15Fe^{2+}{}_{(aq)} + 2SO_4{}^{2-}{}_{(aq)} + 16H^+{}_{(aq)} \quad (3)$$

Visual observations of museum specimens of pyrite of similar age and storage conditions show the mineral can have markedly different appearances, from lustrous to dull and crumbling apart [6]. These observations indicate that different sources of pyrite can undergo oxidation at noticeably different rates [10].

An understanding the nature of the variations in pyrite reactivity is important, for both industrial processing of mineral ores (and wastes) and improving the recovery of refractory gold. Western Australian ores have been reported to contain up to 42% refractory gold (gold that is bound within the sulfide fraction and difficult to extract using traditional cyanide processes). Improvements in understanding the pyrite chemistry may allow industrial processes to be manipulated to increase the recovery of this bound gold [9]. Furthermore the variable reactivity of pyrite has been hypothesised as an underlying cause of variable flotation response in mineral pulps and during sulfide leaching [1]. In addition, mine tailings containing pyrite samples that exhibit greater reaction rates may require more aggressive treatment to reduce the environmental impact of acid mine drainage than those which are less reactive.

Two main factors are hypothesised to affect the reactivity of pyrite; (a) the composition of the mineral, particularly the minor and trace element contents, and (b) the conditions under the pyrite is formed [1]. Although no significant deviations from the stoichiometry of pyrite (1:2, Fe:S) have been reported [1], it has been noted that p-type pyrites are often slightly sulfur rich (as sulfur acts as an electron acceptor) and vice versa for n-type semiconductors which are iron rich [11]. Elements frequently found as impurities in significant quantities (up to a few wt.%) in pyrite can include: Ag, As, Au, Co, Cu, Ni, Sb and Sn. Other elements found in smaller quantities can include Bi, Cd, Hg, Mo, Pb, Pd, Ru, Se, Te, Tl and Zn [1].

* Corresponding author. Tel.: +61 8 82012191; fax: +61 8 82012905.
E-mail address: claire.lenehan@flinders.edu.au (C.E. Lenehan).

0039-9140/$ – see front matter © 2010 Elsevier B.V. All rights reserved.
doi:10.1016/j.talanta.2010.07.086

A survey of the literature reveals relatively few studies concerning this apparent variation in the rate of reactivity of natural pyrites [6,12–17], and the reported results have been mixed. Each of these reports describes different kinetic tests whereby a sample of pyrite is placed in oxidising conditions and one or several of the reaction products (such as pH, sulfate or iron concentration) is monitored over time [18]. However, these tests take a very long time (which can range from days to years) and use very large sample sizes (from tens of grams to thousands of tonnes for larger field tests) [18]. Interpretation and analysis of these results is further complicated by the fact that each study has performed the experiments in a different manner. Inconsistencies in the sample preparation, oxidant used, reaction pH, and progress variable make it difficult to reach any significant conclusions using all the available data.

In order to fully understand the natural variation in pyrite reactivity, experiments on a large number of samples from a wide variety of occurrences must be conducted in a controlled manner where the data collected can be accurately compared. This includes controlling reaction conditions, sample preparation, sample analysis and data handling. Flow injection analysis (FIA) is ideal for this purpose owing to the reproducible timing of sample injection and detection which is inherent to the method [19]. Moreover software used to control an FIA manifold such as LabVIEW® can be employed for the automated but also flexible collection and processing of analytical data [20].

The level of solubilised iron has been reported as a good measure of reaction progress as, unlike sulfur, which has complex speciation and is known to proceed through several intermediate species during the oxidation of pyrite [21], iron's aqueous chemistry is comparatively simple and well understood [22]. Determination of iron in solution can be achieved using a number of well defined methods including colorimetry [23], atomic absorption spectroscopy [23], potentiometry [24], ICP-MS [25] to name a few. In 2002 Karamanev et al. [26] reported the batch determination of ferric and total iron in mine drainage waters using the colorimetric reagent 5-sulfosalicylic acid (SSA) [26]. Under acidic conditions ferric iron reacts with SSA on a 1:1 ratio to form a deep red complex, FeSSA; whilst under basic conditions (pH > 8) ferrous ion is rapidly oxidised to form ferric iron which subsequently complexes with SSA in a 1:3 ratio to form $Fe(SSA)_3$ [27]. The result is an orange coloured solution with a maximum molar extinction coefficient of 5600 M^{-1} cm^{-1} at 420 nm [27].

Importantly, the chemistry is insensitive to interference from oxidising agents and most other metal ions and is relatively unaffected by moderate changes in pH, which is in contrast to the more commonly used 1,10-phenanthroline [23].

This paper presents a flow injection analysis (FIA) method for the determination of iron. The method is applied to the determination of pyrite oxidation rate constants for a series of pyrite samples obtained from diverse geographic locations.

2. Materials and methods

2.1. Instrumentation

All the experiments were undertaken using a flow injection analysis manifold constructed in-house, as depicted in Fig. 1. Control of the pump (Gilson Minipuls 3, John Morris Scientific, Melbourne, Australia), 6-port valve (Valco®, GlobalFIA, Fox Island, WA, USA) and UV–vis detector (SCINCO S-3100 UV–VIS Photo Diode Array Spectrophotometer, DKSH Australia Ltd., Hallam, Australia) was achieved using a desktop computer (Dell Optiplex 755 Intel®Core™2 Duo 2.66 GHz, 1.96 GB RAM, Windows XP Professional SP3) running instrument control and data acquisition software developed in-house within the LabVIEW™ graphical programming package (LabVIEW™ 8.2.1 Professional Development System, National Instruments, Melbourne, Australia). The detector was equipped with a flow through cell (quartz windows, nominal volume 0.720 mL, 10 mm pathlength, Starna Pty. Ltd., NSW, Australia) and the average absorbance across the region 423–427 nm was used as the analytical signal.

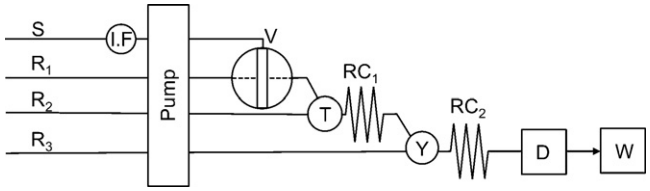

Fig. 1. FIA manifold for the determination of total iron concentration; sample S, 18 Ω water R1, 1.5% (w/w); SSA R2, 2.5% (v/v); ammonia solution R3, 10 μm in-line filter; I.F., injection valve V; reaction coil 1, RC1; reaction coil 2, RC2; T-shaped mixer, T, Y-shaped mixer Y; detector, D; waste, W.

Reagents and samples were propelled by the pump, fitted with 1.02 mm i.d. PVC tubing (DKSH Australia Ltd., Hallam, Australia) at an overall operating flow rate of 5.5 mL min^{-1} (~1.4 mL min^{-1} per line). All the other tubings were 0.5 mm i.d. PTFE (GlobalFIA, Fox Island, WA, USA), with the exception of the tubing connecting junctions T and Y (Fig. 1) and tubing from junction Y to waste both of which were 0.8 mm i.d.. All the tubings were connected using standard fittings (GlobalFIA, Fox Island, WA, USA). The reaction coils had nominal volumes of 170 μL (RC1 a coiled reactor) and 31 μL (RC2 a serpentine reactor). An injection volume of 30 μL was used for all the experiments. During pyrite analysis a 10 μm in-line filter (I.F) was fitted to the sample line S to prevent small particles from blocking the injection valve.

To prevent the precipitation of ferric ions as iron(III) hydroxide (which occurs when pH > 3) the carrier (R1) was first merged with the SSA solution (at "T" in Fig. 1) to form an iron–SSA mixture. The resulting stream was merged with an ammonia stream (at "Y" in Fig. 1) to raise the pH for determination of total iron. Ammonia was chosen in order to reduce the likelihood of precipitation of other metal hydroxides within the flow system.

2.2. Optimisation

Simplex optimisation of SSA, ammonia and carrier stream concentration was performed using Multisimplex version 2.1.3 (Grabitech Solutions AB, 2001) with the objective of optimising peak height and minimising relative standard deviations. Maximum, minimum and optimum trialled concentrations are described in Table 1. All the optimisation was done using 25 mg L^{-1} total iron.

2.3. Reagents

All the solutions were prepared in Barnstead ultrapure water (18 MΩ) unless otherwise specified. 5-Sulfosalicylic acid (Sigma–Aldrich, NSW, Australia) and ammonia (Merck Pty. Ltd., Vic, Australia) solutions were obtained.

Stock iron standards (1000 mg L^{-1} total iron) were prepared by dissolving 4.928 g of ferrous sulfate heptahydrate ($(FeSO_4{\cdot}7H_2O)$, Chem-Supply, South Australia) in 1 L of 1 M sulfuric acid. Stock solutions (1000 mg L^{-1}, SpectrosoL) of copper(II) and zinc(II) nitrates, and arsenic(V) oxide in were obtained from BDH (England). Stock solutions (1000 mgL^{-1}) of nickel(II) nitrate and tin(IV) chloride, were obtained from ACR (Moorooka, Australia). The stock solution (1000 mg L^{-1}) of antimony(III) oxide was obtained from Sharlau (Barcelona, Spain). Stock solutions (1000 mg L^{-1}) of cobalt(II) were prepared by dissolving 0.4938 g of cobalt(II)nitrate hexahy-

Table 1
Range of reagent concentrations investigated during Multisimplex optimisation of FIA method.

	[SSA] % (w/v)	[Ammonia] % (v/v)	[H_2SO_4] (carrier) (M)
Initial concentration	1.5	2.5	0.010
Minimum tested concentration	0.8	1.5	0.000
Maximum tested concentration	2.8	5.8	0.015
Optimum concentration	1.5	2.5	0.000

drate ($Co(NO_3)_2{\cdot}6H_2O$, M&B Ltd., Dagenham, UK) in 100 mL of water.

For oxidation of pyrite samples, 35% (w/w) hydrogen peroxide (Chem-Supply, South Australia) and 98% (w/w) sulfuric acid (Ajax Finechem, NSW, Australia) stock solutions were diluted to the required concentration in ultrapure water.

ICP grade standard solutions of 10 mg L^{-1} iron and indium were obtained from Choice Analytical (NSW, Australia) and were diluted appropriately in 2% (m/v) sulfuric acid solution for inductively coupled plasma mass spectrometry (ICP-MS) analysis.

2.4. Pyrite sample preparation

Pyrite samples were obtained from the mineral collection of the South Australian Museum. The samples were examined for any visible impurities (e.g. quartz), if present these were removed by hand, resulting in a visibly homogeneous sample. For analysis of oxidation rate, samples were prepared immediately before analysis to negate any potential effects of storage. Sample preparation proceeded in the following manner: the sample was crushed in a purpose-built cylindrical tempered steel mortar and pestle. The crushed pyrite was then sieved through stainless steel sieves (Retsch, NSW, Australia) to isolate particles in the size range of; 53 μm < x < 106 μm. This fraction was subsequently mixed with approximately 10 mL of acetone and ultrasonicated for 5 min to dislodge the fine mineral powder that is known to adhere to the grain surfaces during the crushing process and the supernatant discarded. This adhering powder has been identified to cause erroneously high reaction rates due to much larger surface areas available for reaction [28]. The process of adding acetone and ultrasonication was repeated until the supernatant was clear. The samples were subsequently rinsed in 18 MΩ water and swirled in 1 M nitric acid for 1 min, re-rinsed in water and finally rinsed with acetone and dried on a hot plate (less than 50 °C) to ensure all the acetone had been removed.

2.5. Sample analysis

Freshly prepared pyrite (0.10 g) was accurately weighed into a clean 150 mL polystyrene beaker to which an acidic peroxide solution (50 mL of a solution containing 1.0 M sulfuric acid and 2.0 M hydrogen peroxide) was added. Immediately at the time of addition, the FIA instrument was started. The pump circulated the pyrite reaction solution through the injection valve returning the solution to the reaction vessel and the software triggered the manifold to inject 30 μL of the reaction solution every minute for 60 min. Sample reactivity was calculated by discarding the first 10 points (i.e. the first 10 min); this time was allowed for the reaction rate to stabilise. The peak height of the remaining 50 points were each averaged over the three replicates and fitted against a linear regression. A linear regression was found to be the most appropriate fit with R^2 usually greater than 0.9, indicating that the reaction is zero order with respect to production of iron (most likely due to the initial excess of oxidant). This was chosen as very poor regression statistics were observed for other common reaction orders. R^2 values were typically less than 0.8 for 1st order and less than 0.5 for 2nd order kinetics. The slope of the regression line was taken as the rate constant (k).

2.6. Method validation

A sample of pyrite was reacted as described earlier, however in addition to the instrument sampling the solution every minute, 30 μL samples were also taken manually using an automatic pipette (Thermo Scientific, Australia) after reacting for 15, 30, 45 and 60 min. These were diluted to 5 mL in 2% H_2SO_4 and analysed for ^{57}Fe using an Agilent 7500cx ICP-MS (Agilent, Victoria, Australia), utilising the octopole reaction system with helium gas (flow rate 5 mL min^{-1}) to correct for the effects of the interfering species ArOH. Instrumental operating conditions were optimised according to the instruments standard operating procedure for maximum sensitivity.

Solutions were measured against a 200 μg L^{-1} indium internal reference standard. A calibration curve for iron was generated from the signals of seven reference standards prepared with concentrations between 0 and 500 μg L^{-1}.

3. Results and discussion

3.1. Simplex optimisation of reagent concentrations

When one or more variables are dependent on each other univariate optimisations may give misleading results, in this case it is more appropriate to employ a multivariate technique [29]. It was decided to perform a simplex optimisation in this study as the iron–SSA complex formed is dependent on the final pH of the solution, with the optimal final pH being greater than 8 [30]. This is interdependent upon the concentration of the ammonia solution, the sample pH and acidity of the carrier stream. The initial reagent concentrations are described in Table 1 above, and the SSA, ammonia and H_2SO_4 were assigned step sizes of 1.5% (w/w), 2.0% (v/v) and 0.01 M respectively. After 13 trials only the ammonia concentration was shown to have a discernable effect on the signal. Peak height increased with increasing ammonia concentration up to 1.5% (v/v) where the signal plateaued, this corresponds to the reagent having an adequate ammonia concentration to elicit the desired change in pH causing full development of the basic SSA colour. Beyond this concentration (1.5%, v/v) the peak height and % RSD fell did not deviate significantly. In all the cases the % RSD of peak height was below 1.8%.

3.2. Flow rate optimisation

As a result of the data acquisition requirements of our in-house software (slower flow rates resulted in a broader peak that could not be captured in its entirety) flow rate was optimised independently of reagent concentration using a univariate approach. In all the cases, the flow of each reagent was maintained at equivalent rates. The optimised reagent conditions used are described earlier (Table 1). The effect of total flow rate on peak height was studied over the range 3.5–11.5 mL min^{-1}. As can be seen in Fig. 2 the maximum peak height was observed at 4.5 mL min^{-1} beyond which the peak height was observed to decrease with increasing flow rate. The signal at 11.5 mL min^{-1} was approximately 30% lower than that of the maximum. Flow rates less than 4.5 mL min^{-1} and greater than 7 mL min^{-1} resulted in increased

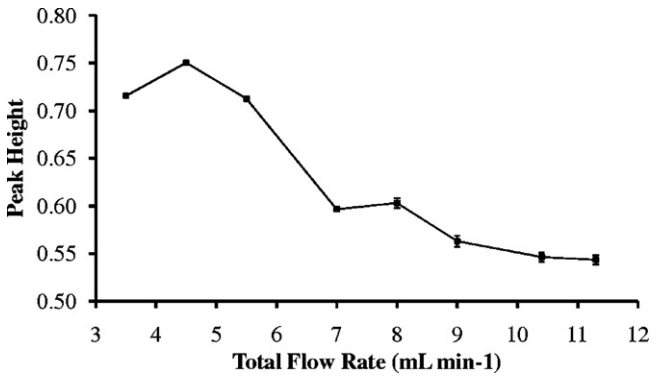

Fig. 2. Effect of flow rate on measured peak height, error bars showing ±1 standard error. Conditions: 150 mg L^{-1} [Fe] 18 MΩ water, 1.5% (w/v) SSA, 1.5 (v/v) ammonia, injection volume 30 μL.

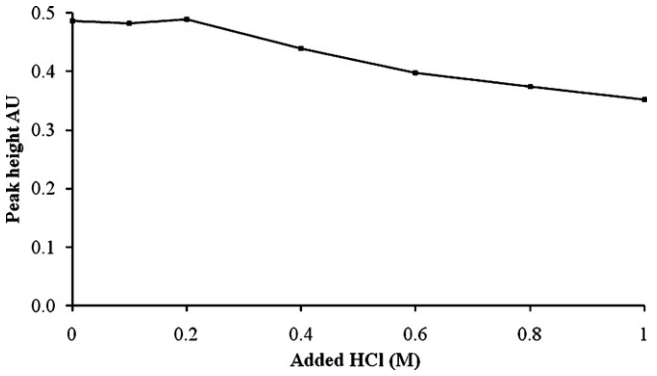

Fig. 3. Effect of increasing acid concentration of sample matrix on peak height. Conditions: 100 mg L^{-1} [Fe], 18 MΩ water, 1.5% (w/v) SSA, 1.5 (v/v) ammonia, flow rate 5.5 mL min^{-1}, injection volume 30 μL.

variability of peak height when compared with flow rates between 4.5 and 7 mL min^{-1}. Furthermore at flow rates below 4.5 mL min^{-1} resulted, very broad peaks and a lower throughput were observed. Consequently we chose a flow rate of 5.5 mL min^{-1} as a compromise between high reproducibility and narrow peak widths, and throughput.

3.3. Calibration

A series of calibration standards were prepared in the region 5–150 mg L^{-1} and analysed using the optimised conditions described earlier. The resulting calibration curve had a linear trendline with the equation: $y = 0.0035x + 0.129$, where y = peak height (AU) and x = iron concentration (mg L^{-1}) and an R^2 value of 0.999. The limit of detection (blank + 3σ) was 0.5 mg L^{-1}. Typical relative standard deviations were less than 2% with the highest relative standard deviation being 2.4% at the 5 mg L^{-1} level (n = 10).

3.4. Interference studies

As pyrite is oxidised (either under the conditions described in this study or in the natural environment) sulfuric acid is formed. This decreases the pH of the surrounding solution. In addition, pyrite can often contain many different elements as mineral inclusions or lattice substitutions which can occur in concentrations of up to several weight percent [1] and these elements would be released into solution. Therefore it is important to know whether varying the acid concentration and trace element composition of the sample matrix will impact the analysis.

In order to determine the effect of additional acid on the system, known volumes of hydrochloric acid was added to the reaction matrix and the peak height for a 100 mg L^{-1} iron solution was monitored. Hydrochloric acid was chosen as it is a strong monoprotic acid and the additional hydronium concentration could be accurately calculated. As can be seen in Fig. 3 the peak height is initially unaffected by increasing the acid concentration (from the original 1 M) of the sample matrix by up to 0.2 M after which there is a steady decrease in signal. The observed decrease in peak height is due to the pH of the analysed solution decreasing to a point where it is too low to evoke the full colour change. For detection of total iron by SSA, a more concentrated ammonia solution would be required.

The addition of several different ions (As^{5+}, Co^{2+}, Cu^{2+}, Ni^{2+}, Sb^{3+}, Sn^{2+} and Zn^{2+}) commonly found as impurities in pyrite were investigated for their effect on the signal peak height. Standard solutions of iron (100 mg L^{-1}) were individually spiked with the interfering ions under investigation and peak heights of the resulting solutions were compared with that of an unspiked iron solution. The results of this study are summarized in Table 2. As shown, with the exception of antimony and zinc, which both resulted in a 5% decrease in signal, the method was not significantly affected by the presence of interferents at a 1:1 mole ratio. Whilst the presence of antimony and zinc resulted in a distinct decrease in absorbance at a 1:1 mole ratio, a 2:1 mole ratio (iron:interferent) did not significantly affect the peak height. It is thought that the decrease in peak height for antimony may simply be due to either the acidic nature of the supplied standard solutions (antimony was prepared in 5 M HCl whilst all the others were prepared in either 0.5 or 1 M acid solutions). These concentrations of interferences would not normally be expected in a pyrite sample, as pyrite is not known to deviate significantly from the 1:2 Fe:S stoichiometry [1] and would normally contain only mg kg^{-1} levels of the cations studied. Therefore when applied to real samples the method is essentially free from interferences.

3.5. Method validation

In order to confirm the results obtained using our colorimetric FIA system, the method for determining total iron was validated against an established ICP-MS method. The concentration of iron was determined for four subsamples of a pyrite oxidation that were taken at the same time as it was sampled for FIA. As can be seen in Fig. 4 the concentrations of iron determined by the two methods correlated very strongly. Linear regressions of each set of data gave equations: $y = 0.011x - 1.60$ and $y = 0.012x - 1.54$ for ICP-MS and FIA respectively.

Table 2
The change in peak height as a % of the unspiked signal ± 1 standard error from a 100 mg L^{-1} Fe solution (average signal 0.46 AU) observed upon the addition of various elements.

Molar ratio (Fe:interferent)	As (% change)	Co (% change)	Cu (% change)	Ni (% change)	Sb (% change)	Sn (% change)	Zn (% change)
1:0.01	0.8 ± 0.2	−1.9 ± 0.1	−2.0 ± 0.2	−0.3 ± 0.1	−3.5 ± 0.5	−1.0 ± 0.2	−0.7 ± 0.2
1:0.1	1.3 ± 0.3	−2.4 ± 0.1	1.3 ± 0.1	−0.5 ± 0.1	0.2 ± 0.2	0.0 ± 0.3	−3.8 ± 0.5
1:0.5	1.1 ± 0.2	−1.6 ± 0.2	0.9 ± 0.2	−0.2 ± 0.2	1.5 ± 0.5	0.9 ± 0.3	−2.1 ± 0.5
1:1	2.2 ± 0.4	0.2 ± 0.1	1.0 ± 0.3	−1.1 ± 0.2	−5.4 ± 0.4	−3.0 ± 0.4	−5.0 ± 0.3

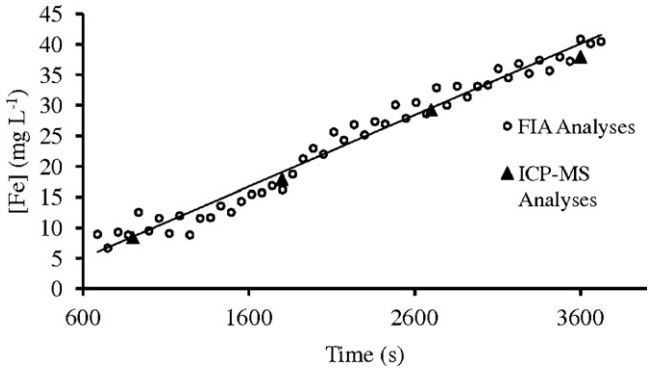

Fig. 4. Comparison of FIA and ICP-MS methods for determination of total iron in solution. Error bars (where visible) show ±1 standard error. Solution from the reaction of 0.1 g pyrite (Isle of Elba) in 2 M H_2O_2 and 1 M H_2SO_4 (50 mL) sampled per minute for FIA and per 15 min for ICP-MS, reactivity = 0.012 mg L^{-1} s^{-1}. FIA conditions: 1 M H_2SO_4 sample matrix, 18 MΩ water, 1.5% (w/v) SSA, 1.5 (v/v) ammonia, flow rate 5.5 mL min^{-1}, injection volume 30 μL.

Table 3
Geological origin and crystal habit of each of the tested pyrite samples.

Sample origin	South Australian Museum Reg No.	Crystal habit
Nairne, Brukunga, South Australia	SAM G16022	Pyritohedral
Poona Mine, Moonta, SA	SAM G17012	Pyritohedral, intergrown with quartz
Gumeracha, SA	SAM G18915	Striated cubic/pyritohedral
Wuxuan, Guangxi, China	SAM G29982	Nodular, radiating (sunflower)
Pacific Ocean	SAM G30334	Massive/granular
Black Cloud Mine, Leadville, CO, USA	SAM G32419	Cubic
Daly-Judge Mine, Peak City, UT, USA	SAM G32420	Pyritohedral
Isle of Elba, Italy	SAM G6876	Pyritohedral
Navajun, Spain	SAM G33033	Cubic
Sparta, Randolph County, IL	SAM G30955	Flattened, nodular (dollar)

3.6. Application to real samples

Pyrite samples from 10 geographical locations were obtained from the South Australian Museum mineral collection (Table 3) and analysed in triplicate using the optimised method as described earlier.

Oxidation rate constants were derived for each sample and are presented in Fig. 5. The samples gave an overall variation in rate constant of (approximately) 0.015 mg L^{-1} s^{-1}, with almost an order of magnitude difference from lowest to highest value. This large difference in reactivity across this relatively small sample set is good preliminary evidence toward the hypothesis that pyrite from different locations do have different inherent reactivities. Further work would include increasing the size of the sample set to more accurately represent the global pyrite population, and also to characterise these samples in terms of impurities and internal texture to see if there is any correlation between the measured difference in reactivity and individual sample attributes.

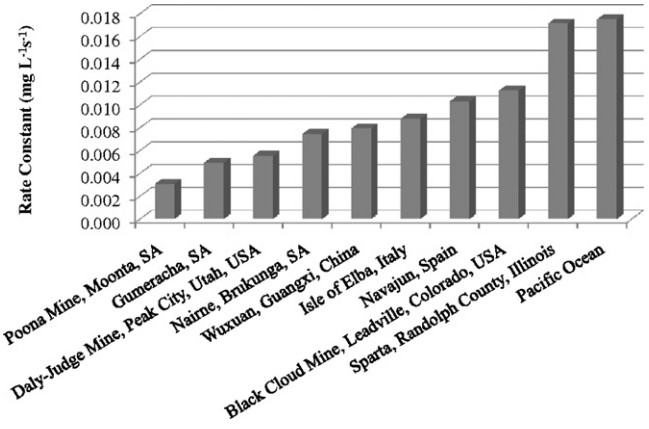

Fig. 5. Relative reactivity rates of 10 pyrite samples.

4. Conclusion

An accurate, reproducible and rapid method for the analysis of total iron in mine drainage water using the colorimetric reagent 5-sulfosalicylic acid in basic conditions has been developed. The method was successfully validated using ICP-MS at several iron concentrations. The method is also suitable for the routine determination of total iron concentration in mine drainage water as well as determination of the reactivity of mineral samples. The method does not suffer from interferences by several metal ions commonly associated with pyrite up to a ratio of 1:1 (molar) though it is sensitive to increases in sample matrix acidity above 0.2 M. The method has been used to collect preliminary data indicating that there is a variation across pyrite minerals from different locations that will provide basis for further investigation.

Acknowledgements

We would like to thank ARC (DP0772229 and DP1095069) for their financial support and Flinders University for a Research Scholarship for OO.

References

[1] P.K. Abraitis, R.A.D. Pattrick, D.J. Vaughan, Int. J. Miner. Process. 74 (2004) 41.
[2] M.M. Antonijevic, M. Dimitrijevic, Z. Jankovic, Hydrometallurgy 46 (1997) 71.
[3] N.O. Egiebor, B. Oni, Asia-Pac. J. Chem. Eng. 2 (2007) 47.
[4] L. Lefticariu, L.M. Pratt, E.M. Ripley, Geochim. Cosmochim. Acta 70 (2006) 4889.
[5] D. Rickard, G.W.I.I.I. Luther, Chem. Rev. 107 (2007) 514.
[6] C.L. Wiersma, J.D. Rimstidt, Geochim. Cosmochim. Acta 48 (1984) 85.
[7] K.S. Savage, D. Stefan, S.W. Lehner, Appl. Geochem. 23 (2008) 103.
[8] P. Chirita, Chem. Biochem. Eng. Q. 21 (2007) 257.
[9] J. Vaughan, JOM J. Min. Met. Mater. Soc. 56 (2004) 46.
[10] A. Newman, The Geological Curator, 6, 1998, p. 363.
[11] D.F. Pridmore, R.T. Shuey, Am. Miner. 61 (1976) 248.
[12] R.M. Garrels, M.E. Thompson, Am. J. Sci. 258A (1960) 56.
[13] R. Liu, A. Wolfe, D. Dzombak, B. Stewart, R. Capo, Environ. Geol. (2007).
[14] R. Liu, A.L. Wolfe, D.A. Dzombak, C.P. Horwitz, B.W. Stewart, R.C. Capo, Appl. Geochem. 23 (2008) 2724.
[15] M. Manaka, J. Min. Petrol. Sci. 102 (2007) 24.
[16] R.V. Nicholson, R.W. Gillham, E.J. Reardon, Geochim. Cosmochim. Acta 52 (1988) 1077.
[17] E.E. Smith, K.S. Shumate, Sulfide to Sulfate Reaction Mechanism, U.S. Federal Water Quality Administration, Washington, 1970.
[18] U.S.E.P.A, Technical Document: Acid Mine Drainage Prediction, U.S. Environmental Protection Agency, 1994.
[19] M.D. Luque de Castro, W. Paul, T. Alan, P. Colin, Encyclopedia of Analytical Science, Elsevier, Oxford, 2005, pp. 31.
[20] C. Wagner, S. Armenta, B. Lendl, Talanta 80 (2010) 1081.
[21] M.J. Borda, D.R. Strongin, M.A. Schoonen, Am. Miner. 88 (2003) 1318.
[22] F. Wisotzky, in: J. Schüring, H.D. Schulz, W.R. Fischer, J. Böttcher, W.H.M. Duijnisveld (Eds.), Redox: Fundamentals, Processes and Applications, Springer, 2000, p. 175.
[23] A.P.H.A., Standard Methods for the Examination of Water and Wastewater, American Public Health Association, Washington, DC, 1998.
[24] W.H. Mahmoud, Anal. Chim. Acta 436 (2001) 199.
[25] J. de Jong, V. Schoemann, J.-L. Tison, S. Becquevort, F. Masson, D. Lannuzel, J. Petit, L. Chou, D. Weis, N. Mattielli, Anal. Chim. Acta 589 (2007) 105.
[26] D.G. Karamanev, L.N. Nikolov, V. Mamatarkova, Miner. Eng. 15 (2002) 341.
[27] I.P. Pozdnyakov, V.F. Plyusnin, V.P. Grivin, D.Y. Vorobyev, N.M. Bazhin, E. Vauthey, J. Photochem. Photobiol. A 181 (2006) 37.
[28] M.A. McKibben, H.L. Barnes, Geochim. Cosmochim. Acta 50 (1986) 1509.
[29] B. Horstkotte, A. Tovar Sanchez, C.M. Duarte, V. Cerda, Anal. Chim. Acta 658 (2010) 147.
[30] I.P. Pozdnyakov, V.F. Plyusnin, N. Tkachenko, H. Lemmetyinen, Chem. Phys. Lett. 445 (2007) 203.